Packet Size Optimization for Lifetime Maximization in Underwater Acoustic Sensor Networks

Huseyin Ugur Yildiz, *Member, IEEE*, Vehbi Cagri Gungor, and Bulent Tavli, *Senior Member, IEEE*

***Abstract*—Recently, underwater acoustic sensor networks (UASNs) have been proposed to explore underwater environments for scientific, commercial, and military purposes. However, long propagation delays, high transmission losses, packet drops, and limited bandwidth in underwater propagation environments make realization of reliable and energy-efficient communication a challenging task for UASNs. To prolong the lifetime of battery-limited UASNs, two critical factors (*i.e.*, packet size and transmission power) play vital roles. At one hand, larger packets are vulnerable to packet errors, while smaller packets are more resilient to such errors. In general, using smaller packets to avoid bit errors might be a good option. However, when small packets are used, more frames should be transmitted due to the packet fragmentation and hence, network overhead and energy consumption increases. On the other hand, increasing transmission power reduces frame errors, but this would result in unnecessary energy consumption in the network. To this end, packet size and transmission power should be jointly considered to improve network lifetime. In this study, an optimization framework via integer linear programming (ILP) has been proposed to maximize network lifetime by joint optimization of transmission power and packet size. In addition, a realistic link-layer energy consumption model is designed by employing physical layer characteristics of UASNs. Extensive numerical analysis through the optimization model has been also performed to investigate the trade-offs caused by the transmission power and packet size quantitatively.**

***Index Terms*—underwater acoustic sensor networks, network lifetime, transmission power control, optimum packet size, integer linear programming.**

I. Introduction

UNDERWATER acoustic sensor networks (UASNs) have drawn a great attraction by researches working on military and commercial aquatic applications. Some use cases of UASNs include oceanic data collection, pollution monitoring, long-term underwater exploration, tactical surveillance, *etc.* [1], [2]. Typical UASNs are formed with numerous sensor nodes that are arbitrarily distributed within a region and a base station (*i.e.*, sink node). Underwater sensor nodes gather data from the underwater habitat and transfer the captured data to the base station generally by using multi-hop communication schemes [3]. Since sensor nodes have scarce battery energy, recharging (or replacing) the batteries of sensor nodes is infeasible [4], [5]. Hence, the optimal utilization of energy consumption becomes an important research challenge in UASNs to attain energy efficiency [6] which yields a prolonged lifetime.

The characteristics of the underwater channel are severe when compared to terrestrial wireless channels. Some notorious features of underwater channels include high path loss (attenuation), frequent packet drops, multi-path fading, dispersion of frequency, limited bandwidth (usually a few kHz), and long propagation delay caused by the speed of sound in water when considering large-scale UASNs [7]. There are several approaches to combat against the crucial nature of the underwater environment to maximize the network lifetime. Two possible solutions are packet size optimization (PSO) as well as transmission power control (TPC) according to the channel conditions.

PSO has proven to have a great impact on the performance of UASNs [8]. Usage of larger frames is an acceptable option as long as the acoustic link quality is sufficient [9]. On the other hand, when channel conditions become harsh which is a frequent occurrence in underwater channels [1], usage of smaller frames are favorable to reduce the frame error rates [10]. However, the price paid for this case is the extra data traffic injected through the network which leads to an overhead of energy dissipation [11]. Although reducing individual frame error rates is critical, data exchange may be performed through a handshaking mechanism [12], [13]. A possible method to perform handshaking is to notify the sender as long as the transmitted data packet is successfully received by using a small-sized acknowledgement (ACK) packet [14]. In such a case, minimizing the handshaking failure becomes more important than minimizing the individual frame errors.

The other important technique to elongate the network lifetime is to utilize TPC schemes [15], [16]. Larger packets which are susceptible to errors require less energy for communications while smaller packets that are resilient to errors need more energy (due to the overhead data generated by fragmentation). Increasing the transmission power helps to minimize the handshaking errors but this method degrades the network energy efficiency. Adjusting transmission powers, according to the requirements of a UASN application, can be either applied at network-level (*i.e.*, usage of a global transmission power at all links) or at link-level (*i.e.*, carefully adjusting the transmission power at each link by considering

H. U. Yildiz is with TED University, 06420, Ankara, Turkey (e-mail: hugur.yildiz@tedu.edu.tr).

V. C. Gungor is with Abdullah Gul University, 38039, Kayseri, Turkey (e-mail: cagri.gungor@agu.edu.tr).

B. Tavli is with TOBB University of Economics and Technology, 06560, Ankara, Turkey (e-mail: btavli@etu.edu.tr).

the conditions of the link) [14]. Hence, determining the optimum transmission power with packet size rises a trade-off which should be carefully addressed for prolonging the lifetime of UASNs.

To address these challenges, we propose a novel optimization model based on integer linear programming (ILP) to jointly explore the effects of PSO and TPC on network lifetime. In summary, our contributions can be listed as follows:

1) We develop a realistic link-layer handshake scheme [12], [17]–[19] which uses foundations of the well studied physical-layer models for underwater communications [20], [21].
2) The proposed link-layer model adopts the power consumption characteristics of widely used six different commercial and experimental underwater modems (*i.e.*, Evo-Logics S2CR 18/34 WiSE, WHOI Micromodem, Teledyne Benthos ATM9XX, LinkQuest UWM4000, Aquatech AQUAModem 1000, and DSPComm AquaComm Marlin [22]).
3) We built a novel optimization framework via ILP that employs the principles of the proposed link-layer model aiming to determine the maximum lifetime of a UASN by jointly considering the PSO and TPC.
4) We investigate the impact of network-level and node-level TPC strategies on the determination of the optimum packet size by using the novel ILP framework through the numerical evaluations.
5) We also determine the optimum packet sizes for several commercial & experimental underwater modems when considering different networking conditions.

The structure of this paper is provided as follows. Section II overviews the literature on PSO in UASNs. In Section III, constructed physical, link-layer, and optimization models are introduced along with proposed TPC approaches. Results of the numerical analysis are provided in Section IV. Finally, Section V provides outcomes of this paper.

II. Related Work

The last two decades have seen a growing trend towards PSO in sensor networks. Some practical use cases of PSO include terrestrial wireless sensor networks (WSNs) [23], [24], cognitive radio sensor networks [25], wireless body area sensor networks [26], terrestrial sensor network based smart grid applications [27], and underground sensor networks [10]. Recently, we observe a growing body of literature on PSO in UASNs [3], [8]–[11], [18], [19], [28]–[33]. We present an overview of the literature on PSO in UASNs as follows.

Stojanovic [8] uses PSO to maximize the throughput efficiency at the link-layer. However, this work ignores the overhead caused by retransmissions or forward error correction (FEC) schemes. Xie and Cui [18] compare the random access and handshaking based methods on the determination of the optimum packet size. In [28] two distributed algorithms are proposed to maximize the energy efficiency and determine the optimum packet size for data gathering applications in UASNs. The impact of PSO on throughput for the MACA-U protocol (*i.e.*, underwater adaptation of the MACA protocol [17]) is elaborated in [19]. A cross-layer examination of PSO is performed for terrestrial, underwater, and underground sensor networks in [10] by incorporating FEC methods. Basagni *et. al.* [29] provide a comprehensive analysis to quantify the effects of PSO on throughput, latency, and energy-per-bit consumption for different link-layer protocols. They also study the benefits of PSO and usage of packet fragmentation in harsh environments in [30]. Besides, the authors incorporate the effects of interference and varying bit error rates in [3]. PSO and energy efficiency issues in conjunction with FEC for shallow water acoustic channels are investigated in [31]. The relationship between the optimum packet size, throughput, and packet errors by considering a two-hop ACK model is studied in [9]. Ahmad *et. al.* [11] determine the optimum packet size by considering the environmental factors such as temperature, pressure, salinity, *etc.* In [32] the impact of PSO on the throughput of a link that is affected by mobility is investigated. In [33] authors propose an optimization model for energy efficiency that can satisfy both a given signal-to-noise ratio (SNR) at the physical layer as well as throughput at the link-layer.

As a summary, the key performance metrics for PSO in UASNs can be categorized as: throughput [3], [8], [10], [11], [18], [19], [29], [30], [32], [33], latency [3], [9], [10], [29], [30], energy efficiency [3], [10], [28]–[31], and packet error rate [3], [9], [10], [28]–[31].

Recent advancement of sensor node hardware technology enables intelligent TPC mechanisms to be used for reducing the overall energy consumption in the network. One way of using TPC is to devise a sleep/awake scheduling [7]. The other way is to adjust transmission power according to the channel conditions. Considering the second case, adjustment of transmission power can be applied at network-level or at link-level [14] as stated in the introduction section. Although consolidation of PSO and TPC are efficient ways to maximize the network lifetime, researchers should also put a special emphasis to ensure collision-free data exchanges to satisfy a predetermined quality of service in UASNs. Two promising methods to fight against collisions are the random access [34] and handshaking [12], [13]. In random access, the transmitter sends packets without any coordination hence packet avoidance occurs in a probabilistic manner [18]. On the other, handshaking based protocols use small packets (*i.e.*, request-to-send (RTS) and clear-to-send (CTS)) before the data exchange starts to avoid collisions [12], [19]. Although the high propagation delay degrades the performance of handshaking in UASNs, this approach still can be used by utilizing an idle/wake (or a sleep/wake) mechanism for low-duty-cyle applications [34] such as the network lifetime maximization problem as explored in this study. Moreover, it is shown that handshaking can perform better results in many UASN applications [18].

The closest study to ours is [27] where the impact of PSO and TPC on terrestrial WSNs deployed in smart grid environments are investigated through an optimization model. Indeed, optimization model in this paper is inspired by the model in [27]. However, there are many significant differences between [27] and this study. First, in [27] investigates terrestrial WSN based smart grids whereas this study is on UASNs.

Second, the channel model in [27] is a log-normal shadowing based wireless channel model where the shadowing component is modeled as a Gaussian random variable and the mean and variance of this random variable are derived experimentally, however, in this study, we adopt both an empirical model (*i.e.*, Urick's model) and an accurate ray tracing model (*i.e.*, BELLHOP model) to correctly model the complex nature of the underwater channel. Third, in [27] only a specific platform (*i.e.*, Tmote Sky) is modelled, yet, in this work, we consider a total of six different commercial and research underwater modems (*i.e.*, EvoLogics S2CR 18/34 WiSE, WHOI Micro-modem, Teledyne Benthos ATM9XX, LinkQuest UWM4000, Aquatech AQUAModem 1000, and DSPComm AquaComm Marlin).

Although PSO and TPC issues are studied extensively in terrestrial sensor networks, our work differs from these studies such that we propose a realistic link-layer model that incorporates characteristics of underwater propagation, communication & power control techniques, and power consumption characteristics of different underwater modem platforms. In addition, there have been no studies in the literature on joint optimization of transmission power and packet size to prolong UASN lifetime by using a realistic link-layer model.

III. System Model

In this section, we introduce the abstraction for the energy dissipation in the network which is built onto a realistic physical model for UASNs; then we present our optimization framework that aims to maximize the network lifetime. In this section we use power consumption characteristics of EvoLogics S2CR 18/34 WiSE underwater modem [35] which operates in 18–34 kHz frequency band with a central operating frequency as $f = 26$ kHz. The reported electrical transmission powers for EvoLogics S2CR 18/34 WiSE are in the interval 2.8–35 W. For the sake of simplicity we define set $\mathcal{L} = \{5, 10, 15, \ldots, 35\}$ to represent discrete transmission power levels used throughout this work. In the analysis section (*i.e.*, Section IV), we also consider the energy dissipation characteristics of several other underwater modems available on the market and academia.

A. Physical Layer Model

We use the principles of the underwater acoustic path loss model (*i.e.*, Urick's model) presented in [21]. The path loss (attenuation) of the acoustic link-(i, j) (*i.e.*, $A_{ij}(f)$) in terms of dB is given by

$$A_{ij}(f)[\text{dB}] = 10\kappa \log_{10}(1000 \times d_{ij}) + d_{ij}a(f)[\text{dB/km}], \quad (1)$$

where f is the central operating frequency (*i.e.*, $f = 26$ kHz for the S2CR 18/34 WiSE modem [35]), $\kappa = 2$ is the spreading factor accounted for the deep water spherical loss, d_{ij} is the distance of link-(i, j) in km, and $a(f)$ is the absorption coefficient (in dB/km) that is obtained by using the following Thorp's empirical formula [21]

$$a(f)[\text{dB/km}] = \frac{0.11f^2}{1+f^2} + \frac{44f^2}{4100+f^2} + 2.75 \cdot 10^{-4} f^2 + 0.003. \quad (2)$$

The ambient noise consists of turbulence $N_{\text{t}}(f)$, shipping $N_{\text{s}}(f)$, wind-driven waves $N_{\text{w}}(f)$, and thermal noise $N_{\text{th}}(f)$. These individual noise components can be calculated (in dB re 1μPa per Hz) as follows [21]

$$\begin{aligned} 10\log_{10} N_{\text{t}}(f) &= 17 - 30\log_{10} f, \\ 10\log_{10} N_{\text{s}}(f) &= 40 + 20(s - 0.5) + 26\log_{10} f \\ &\quad - 60\log_{10}(f + 0.03), \\ 10\log_{10} N_{\text{w}}(f) &= 50 + 7.5\sqrt{w} + 20\log_{10} f \\ &\quad - 40\log_{10}(f + 0.4), \\ 10\log_{10} N_{\text{th}}(f) &= -15 + 20\log_{10} f. \end{aligned} \quad (3)$$

Hence, we can express the total noise power density in linear scale as $N(f) = N_{\text{t}}(f) + N_{\text{s}}(f) + N_{\text{w}}(f) + N_{\text{th}}(f)$, where $s = 0.5$ denotes a medium shipping activity factor and $w = 5$ is the wind speed in m/s.

By using the passive sonar equation [36], the SNR at node-j due to the transmission of node-i with power level-l (*i.e.*, $l \in \mathcal{L}$) is expressed as

$$\text{SNR}_{ij}(l, f)[\text{dB}] = P_{tx}^{ac}(l) - N(f)[\text{dB}] - A_{ij}(f)[\text{dB}], \quad (4)$$

where $P_{tx}^{ac}(l)$ is the transmit sound source level at power level-l (in dB re 1μPa). The electrical transmit power level-l in terms of watts, $P_{tx}^{el}(l)$, can converted to dB re 1μPa as [36]

$$10\log_{10} P_{tx}^{el}(l) = 10\log_{10} P_{tx}^{ac}(l) - 170.8 - 10\log_{10}\xi, \quad (5)$$

where 170.8 dB accounts for the conversion from dB re 1μPa to Watts, and $\xi = 0.8$ is the efficiency of the transducer. We assume the binary phase shift keying (BPSK) as the modulation scheme where the probability of a successful M-byte frame reception at node-j that is transmitted from node-i by using the power level-l, is given as [37]

$$\rho_{ij}^{s}(l, f, M) = \left(1 - \frac{1}{2}\text{erfc}\sqrt{\text{SNR}_{ij}(l, f)\frac{B_N}{R}}\right)^{8\times M}, \quad (6)$$

where $B_N = 1$ kHz is the noise bandwidth, $R = 13.9$ kbps is the data rate of the S2CR 18/34 WiSE modem [35], and $\text{SNR}_{ij}(l, f)$ is in linear scale. Similarly, the packet error rate is calculated as $\rho_{ij}^{f}(l, f, M) = 1 - \rho_{ij}^{s}(l, f, M)$. Since we consider a fixed central frequency of operation, we omit the f notation throughout this paper.

Urick's model is a rough approximation for the path loss analysis hence practical applications based on this model may provide misleading results. In order to rigorously assess the complex physical layer conditions of a UASN, more accurate tools that can perform ray tracing should be used. One of the most popular ray tracing tools used in the UASN literature is called BELLHOP model that is designed to perform acoustic ray tracing for a given speed of sound profile and absorbing boundary conditions [20]. BELLHOP model produces ray coordinates, acoustic pressure, or transmission loss values as outputs [38]. Many of today's popular simulators such as SUNSET [39] and DESERT [40] have adopted both Urick and BELLHOP models in their libraries. BELLHOP model has proven to be an accurate physical model tool for underwater communications operating at frequencies which are greater than 1 kHz [41], [42]. In the analysis section results will

be presented for both Urick and BELLHOP models. For the BELLHOP model we adopt the parameters given in [41] such that we utilize an iso-speed sound velocity profile (*i.e.*, $c = 1500$ m/s) and bottom sound speed is taken as $c_b = 1800$ m/s. We also assume that sea surface and floor are flat and densities of the seawater and bottom are taken as $\rho_s = 1024$ and $\rho_b = 1843\ kg/m^3$, respectively.

B. Link-Layer Model

In this section, we describe our link-layer model which uses a slotted (rounded) communication scheme where each round is defined as 150 seconds. We define s_i to represent the number of data frames generated at each round. In this work, we consider an underwater surveillance scenario where each node is equipped with an onboard camera that captures an image of 512×512 pixels of image with 8 bits per pixel at each round. The raw image is assumed to be compressed by using JPEG-2000 with 0.01 compression rate which yields 2603 bytes of processed image data [43]. For the sake of simplicity, we assume that $L_D = 3000$ bytes of image data are acquired by the sensor nodes which are indented to be transferred to the base station at each round. We denote the payload size with L_{PL} which can take one of the following: 3000, 1500, 750, 600, 500, 375, 300, 250, 200, 150, 100, 75, 50, and 30 bytes. Hence if the payload size is adjusted as 3000 bytes, the sender node will transmit a single data frame (*i.e.*, $s_i = L_D/L_{PL} = 1$). However, if 30 bytes of payload trunk is used, then the sender node transmits 100 data frames (*i.e.*, $s_i = 100$). This idea is valid for other payload sizes. The data frame has an additional 20-byte of header information ($L_H = 20$ bytes). Thus the data frame size is calculated by $L_P = L_{PL} + L_H$ bytes. $L_A = 20$ bytes denotes the length of an ACK packet.

We define the active slot time of link-(i,j) as $t^s_{ij} = t(L_P) + t(L_A) + t^p_{ij} + t_g$. In this equation, $t(L_P)$ and $t(L_A)$ are times to transmit a data and an ACK frame. $t^p_{ij} = 2 \times \frac{d_{ij}}{c}$ is the round-trip propagation delay of link-(i,j). t_g is defined as the guard time duration which is used to avoid collision during transmission [44] and taken as twice the maximum propagation delay (*i.e.*, $2 \times \max_{(i,j)}(t^p_{ij})$) [34]. Time slots are cushioned by guard times from both ends to prevent synchronization errors.

While achieving a handshake with success, three possible cases may occur which are enumerated below.

(i) *Successful Handshake:* Data and ACK frames are error-free received at the intended nodes.

(ii) *Unsuccessful Handshake – Case I:* Data frame can be received with no errors in the forward acoustic link, but ACK frame may be dropped in the reverse acoustic channel.

(iii) *Unsuccessful Handshake – Case II:* Data frame may be dropped in the forward acoustic link so that no ACK frames are transmitted in the reverse acoustic channel.

For unsuccessful handshake cases, a retransmission should be initiated to guarantee a successful data and ACK exchange.

Considering the basic handshaking mechanism stated above, if a sender node-i transmits a data frame with the power level-l and receives an ACK packet which is transmitted by the receiver node-j upon receiving the data packet with the power level-k, the probability of successful handshake can be calculated as

$$\rho^s_{HS,ij}(l,k) = \rho^s_{ij}(l, L_P) \times \rho^s_{ji}(k, L_A). \tag{7}$$

On the contrary, handshake error probability is $\rho^f_{HS,ij}(l,k) = 1 - \rho^s_{HS,ij}(l,k)$. If we consider a stop-and-wait automatic repeat request scheme for retransmissions [17], we need to transmit each data packet $\lambda^{lk}_{ij} = 1/\rho^s_{HS,ij}(l,k)$ times on the average.

1) Energy Consumption of the Transmitting Node: If the handshake is successful as stated in case (i), the transmitter side consumes $P^{el}_{tx}(l) \times t(L_P)$ J for data transmission by using power level-l and $P_{rx} \times t(L_A)$ J for ACK frame reception where $P_{rx} = 1.3$ W is the reception power [35]. In the remaining slot time (*i.e.*, $\{t^s_{ij} - t(L_P) - t(L_A)\}$), the transmitter side would be in standby mode where $P_{std} \times \{t^s_{ij} - t(L_P) - t(L_A)\}$ J of energy is dissipated. Note that, $P_{std} = 2.5$ mW is the power expenditure for the standby mode [35]. Hence the total energy dissipation for this case is

$$E^s_{tx,ij}(l,k) = \big[P_{std}\{t^s_{ij} - t(L_P) - t(L_A)\} + P^{el}_{tx}(l)t(L_P) + P_{rx}t(L_A)\big] \times \frac{\rho^s_{ij}(l, L_P)\rho^s_{ji}(k, L_A)}{\rho^s_{HS,ij}(l,k)}. \tag{8}$$

On the other hand, if the handshake is unsuccessful as stated in case (ii), the transmitter side dissipates $P^{el}_{tx}(l) \times t(L_P)$ J for data transmission. Since the ACK frame is dropped due to the channel conditions, the transmitter side does not dissipate energy for ACK reception. Instead, the transmitter will be in the standby mode in the rest of the slot time (*i.e.*, $\{t^s_{ij} - t(L_P)\}$). The energy dissipation in this case will be multiplied by a factor of $[\rho^s_{ij}(l, L_P) \times \rho^f_{ji}(k, L_A)]/\rho^s_{HS,ij}(l,k)$ considering retransmissions. Hence, the energy dissipation for this case is

$$E^{f,1}_{tx,ij}(l,k) = \big[P_{std}\{t^s_{ij} - t(L_P)\} + P^{el}_{tx}(l)t(L_P)\big] \times \frac{\rho^s_{ij}(l, L_P)\rho^f_{ji}(k, L_A)}{\rho^s_{HS,ij}(l,k)}. \tag{9}$$

For the unsuccessful handshake case (iii), the transmitter side still consumes $P^{el}_{tx}(l) \times t(L_P)$ J for data transmission. But the data packet is dropped and the receiver side will not send any ACK frame back to the intended node. The total energy consumption in this case by considering the retransmission factor of $\rho^f_{ij}(l, L_P)/\rho^s_{HS,ij}(l,k)$ is defined as

$$E^{f,2}_{tx,ij}(l,k) = [P_{std}\{t^s_{ij} - t(L_P)\} + P^{el}_{tx}(l)t(L_P)] \times \frac{\rho^f_{ij}(l, L_P)\overbrace{[\rho^s_{ji}(k, L_A) + \rho^f_{ji}(k, L_A)]}^{=1}}{\rho^s_{HS,ij}(l,k)}. \tag{10}$$

In total, the transmitter node spends $E^{tx}_{ij}(l,k) = E^s_{tx,ij}(l,k) + E^{f,1}_{tx,ij}(l,k) + E^{f,2}_{tx,ij}(l,k)$ J of energy.

2) Energy Consumption of the Receiving Node: For the receiver side when we consider the successful handshake (*i.e.*, handshake case (i)), $P_{rx} \times t(L_P)$ J of energy is dissipated for data reception, $P_{tx}^{el}(k) \times t(L_A)$ J for ACK transmission with power level-k, and $P_{std} \times \{t_{ji}^{s} - t(L_P) - t(L_A)\}$ J for standby, respectively. Thus, the total energy expenditure for this case is

$$E_{rx,ji}^{s}(l,k) = \big[P_{std}\{t_{ji}^{s} - t(L_P) - t(L_A)\} + P_{tx}^{el}(k) \\ t(L_A) + P_{rx}t(L_P)\big] \times \frac{\rho_{ij}^{s}(l,L_P)\rho_{ji}^{s}(k,L_A)}{\rho_{HS,ij}^{s}(l,k)}. \tag{11}$$

For the unsuccessful handshake case (ii), the energy cost for successful data packet reception is $P_{rx} \times t(L_P)$. The ACK packet is transmitted with power level-k which costs $P_{tx}^{el}(k) \times t(L_A)$ J of energy. At the rest of the slot time, the receiving node switches to standby mode which requires $P_{std} \times \{t_{ij}^{s} - t(L_P) - t(L_A)\}$ J of energy. Hence, the total energy consumption including retransmissions can be obtained as

$$E_{rx,ji}^{f,1}(l,k) = \big[P_{std}\{t_{ji}^{s} - t(L_P) - t(L_A)\} + P_{tx}^{el}(k)t(L_A) \\ + P_{rx}t(L_P)\big] \times \frac{\rho_{ij}^{s}(l,L_P)\rho_{ji}^{f}(k,L_A)}{\rho_{HS,ij}^{s}(l,k)}. \tag{12}$$

For the unsuccessful handshake case (iii), the receiving node cannot receive the transmitted data, hence in whole slot time the receiving node is in standby mode. The total energy dissipation for this case is

$$E_{rx,ji}^{f,2}(l,k) = P_{std} \times t_{ji}^{s} \times \frac{\rho_{ij}^{f}(l,L_P)}{\rho_{HS,ij}^{s}(l,k)}. \tag{13}$$

In overall, the receiving node consumes $E_{ji}^{rx}(l,k) = E_{rx,ji}^{s}(l,k) + E_{rx,ji}^{f,1}(l,k) + E_{rx,ji}^{f,2}(l,k)$ J of energy.

C. Optimization Model to Maximize the Network Lifetime

In this part, we present our optimization framework given in Figure 1 with the objective function of maximizing the network lifetime. Our proposed framework is constructed by using ILP. The UASN that we consider in this work is denoted as $G(V,E)$ where V is the set of all nodes while we define set W to stand for the acoustic sensor nodes. The base station is marked as node-1. E is the directed link set. We assume that a sensor node cannot transmit data to itself and base station cannot generate data. Our decision variable is denoted with an integer variable f_{ij} which translates to the number of frames transmitted from node-i to node-j. We organize network lifetime (*i.e.*, N_R) with rounds and assume that each round lasts 150 seconds (*i.e.*, $T_R = 150$ s). The network lifetime is defined as the time until the first node depletes its all battery energy [7]. $E_{ij}^{tx}(l,k)$, $E_{ji}^{rx}(l,k)$, and λ_{ij}^{lk} parameters are imported from the preceding subsection.

The constraints of the ILP model are defined in 14–19. Constraint 14 is defined for *flow balancing* which states that for each sensor node (*i.e.*, $\forall i \in W$), incoming traffic (*i.e.*, $\sum_{j \in W} f_{ji}$) plus traffic generated during the lifetime (*i.e.*, $N_R \times s_i$) is equal to the outgoing traffic ($\sum_{j \in V} f_{ij}$). We define Constraint 15 to ensure that all acquired data to be collected at the base station. Constraint 16 is the *energy balancing* constraint that limits the amount of energy consumed for transmission (*i.e.*, $\sum_{j \in V} E_{ij}^{tx}(l,k)f_{ij}$) and reception (*i.e.*, $\sum_{j \in W} E_{ji}^{rx}(l,k)f_{ji}$) to the initial battery energy (*i.e.*, ϱ) at each sensor node. Note that the energy cost for transmission and reception dominates the total energy dissipation in UASNs [36]. For a Lithium battery with 25 V of voltage and 119 Ah

Maximize N_R
Subject to:

$$\sum_{j \in V} f_{ij} - \sum_{j \in W} f_{ji} = N_R \times s_i \ , \forall i \in W \tag{14}$$

$$\sum_{(j,1) \in E} f_{j1} = N_R \sum_{j \in W} s_j \tag{15}$$

$$\sum_{j \in V} E_{ij}^{tx}(l,k)f_{ij} + \sum_{j \in W} E_{ji}^{rx}(l,k)f_{ji} \leq \varrho \ , \forall i \in W \tag{16}$$

$$8 \times (L_P + L_A) \times \left(\sum_{j \in V} f_{ij}\lambda_{ij}^{lk} + \sum_{j \in W} \lambda_{ji}^{lk} f_{ji} \right) = \chi_i, \quad \forall i \in V \tag{17}$$

$$\chi_i \leq N_R \times T_R \times R \ , \forall i \in V \tag{18}$$

$$f_{ij} \geq 0 \ , \forall (i,j) \in E \tag{19}$$

Fig. 1: The ILP model that maximizes network lifetime

TABLE I: Simulation parameters.

Channel Parameters		
κ	Spreading factor	2
B_N	Noise bandwidth (kHz)	1
c	Nominal speed of sound in water (m/s)	1500
c_b	Bottom sound speed (m/s)	1800
ρ_s	Seawater density (kg/m^3)	1024
ρ_b	Seabottom density (kg/m^3)	1843
Packet Parameters		
L_A	ACK size (bytes)	20
L_D	Amount of data generated at each round (bytes)	3000
L_H	Header size (bytes)	20
L_{PL}	Payload size (bytes)	3000, 1500, 750, 600, 500, 375, 300, 250, 200, 150, 100, 75, 50, and 30
s_i	Number of data frames generated at each round	1, 2, 3, 4, 5, 6, 8, 10, 12, 15, 20, 30, 40, 50, 60, and 100
Network Parameters		
$\|V\|$	Number of nodes including the base station	50, 100, 200
h	Node depth (m)	500, 1000, 3500
R_{net}	Network radii (km)	14, 16, 18, 20
T_R	Round duration (s)	150
ϱ	Initial battery energy (MJ)	10,7
# of random topologies		200

charge capacity, ϱ can be calculated as 10.7 MJ [45]. It is noteworthy to state that the base station does not have such a constraint. We assume that if a node is not in the transmitting, receiving, or standby state, the node can shutdown itself by using a wake up module [35]. Constraint 17 is expressed to calculate the *bandwidth required* (*i.e.*, χ_i – in terms of bits) at each node (including the base station) considering both transmission, reception, and retransmissions. With the help of Constraint 18, we limit the bandwidth utilization to $N_R \times T_R \times R$ (total amount of available bandwidth in terms of bits). Finally, Constraint 19 shows the boundaries of our decision variables.

D. Proposed TPC Approaches

In this subsection we present the network-level and link-level TPC strategies which are constructed by using the optimization model presented in the previous subsection. We aim to quantify the impact of TPC strategies on the optimum packet size and the network lifetime.

1) Network-Level Transmission Power Control (NL-TPC): The network-level TPC approach is straightforward such that a single global transmission power level (*i.e.*, l) is utilized in all links for both data and ACK packet transmissions. We can mathematically model NL-TPC approach as

$$l_{ij}^{opt} = k_{ji}^{opt} = l, \quad \forall (i,j) \in E. \tag{20}$$

Note that, in the above equation l_{ij}^{opt} denotes the data power level used on link-(i,j) while k_{ji}^{opt} models the ACK transmission power level in the reverse link (*i.e.*, link-(j,i)).

2) Link-Level Transmission Power Control (LL-TPC): We employ the link-level TPC approach as stated in Equation 21 [14]. The idea is to choose best power levels l_{ij}^{opt} and k_{ji}^{opt} for each data and ACK frames on each link-(i,j) such that the total energy dissipation for transmission and reception on link-(i,j) (given as $E_{ij}^{tx}(l,k) + E_{ji}^{rx}(l,k)$) is minimized.

$$\{l_{ij}^{opt}, k_{ji}^{opt}\} = \underset{l \in \mathcal{L}, k \in \mathcal{L}}{\operatorname{argmin}} \left(E_{ij}^{tx}(l,k) + E_{ji}^{rx}(l,k) \right). \tag{21}$$

IV. Analysis

In this section, we present the results of our investigation on PSO jointly with TPC for maximizing the UASN lifetime. We construct our physical model (Section III-A) and link-layer model (Section III-B) in MATLAB while the optimization model (Section III-C) is built and solved by using GAMS with CPLEX solver. Throughout the analysis section, we investigate the impact of NL-TPC and LL-TPC approaches jointly on network lifetime and optimum frame size in Sections IV-A and IV-B, respectively. We compare the lifetimes for these approaches in Section IV-C. Furthermore, determination of optimum frame size for several commercial & research underwater modems are presented in Section IV-D. Finally, in Section IV-E we exactly and heuristically solve the optimization model and provide a comparative analysis on both lifetimes and solution times. Table I shows the parameters used throughout the analysis.

In this study, we construct an optimization framework based on ILP, and our analyses are performed through the numerical solutions of our model for a wide range of problem instances. Therefore, utilization simulators specifically designed for underwater networks cannot be employed in the solution of the optimization models.

We model our network as a static three-dimensional UASN [1] where 49 sensor nodes (*i.e.*, $|W| = 49$) are mounted on the bottom of the ocean [46] with the depth of 1 km (*i.e.*, $h = 1000$ meters). Since we are working in a deep water channel, effects of multi-path are neglected [15]. At the bottom of the ocean, the network deployment area is considered as a disk of radius R_{net} such that sensor nodes are randomly deployed (according to a uniform distribution) within the disk. The base station is mounted under a floating surface station located at the center of the disk which is anchored to the bottom of the ocean. Hence the total number of nodes in the network is $|V| = |W| + 1 = 50$. We assume that coordinates of nodes (including the base station) do not change in time. We choose several R_{net} values (*e.g.*, 14, 16, 18, and 20 km) to examine the impact of node density on the UASN lifetime. Note that we choose these R_{net} values to work in an extreme underwater environment where the average successful handshake probability values lie within 0.09–0.23. Each data point presented in the subsequent figures is the average of 200 random topologies so that we have the opportunity to analyze the influence of topological changes. Furthermore, for each curve in Figures 2–5 we present normalized lifetime values which are obtained by dividing the absolute lifetime values (for each payload size) to the maximum lifetime value (which is obtained with the payload size that yields a maximum lifetime). In the rest of this manuscript, payload sizes are provided in descending order (*i.e.*, 3000, 1500, 750, 600, 500, 375, 300, 250, 200, 150, 100, 75, 50, and 30 bytes) because we are dealing with s_i (*i.e.*, number of data frames produced at each round) given in ascending order (*i.e.*, 1, 2, 3, 4, 5, 6, 8, 10, 12, 15, 20, 30, 40, 50, 60, and 100).

The lifetime maximization problem that we are investigating in this work has known to have convergecast traffic (*i.e.*, all traffic terminates at the base station) [27]. In addition, with the help of the retransmissions, we assume that all generated data by sensor nodes successfully conveyed to the base station. Nevertheless, the networking mechanism that ILP model employs at each round is that every sensor nodes generates $L_D = 3000$ bytes of data which are either fragmented or not; that are successfully conveyed to the base station with the help of retransmissions. Data exchange among nodes requires both transmission and reception energy dissipations which lessens the remaining battery energy. As the first sensor node depletes its initial battery, the number of rounds that network survives (*i.e.*, N_R) yields the lifetime. The same optimal flow pattern is used for the rest of the rounds in order to maximize the network lifetime. The end-to-end latency for a single sensor node to transmit its own data to the base station is upper bounded by T_R seconds which is the round duration. In order to see this result, we divide both sides of Constraints 17 and

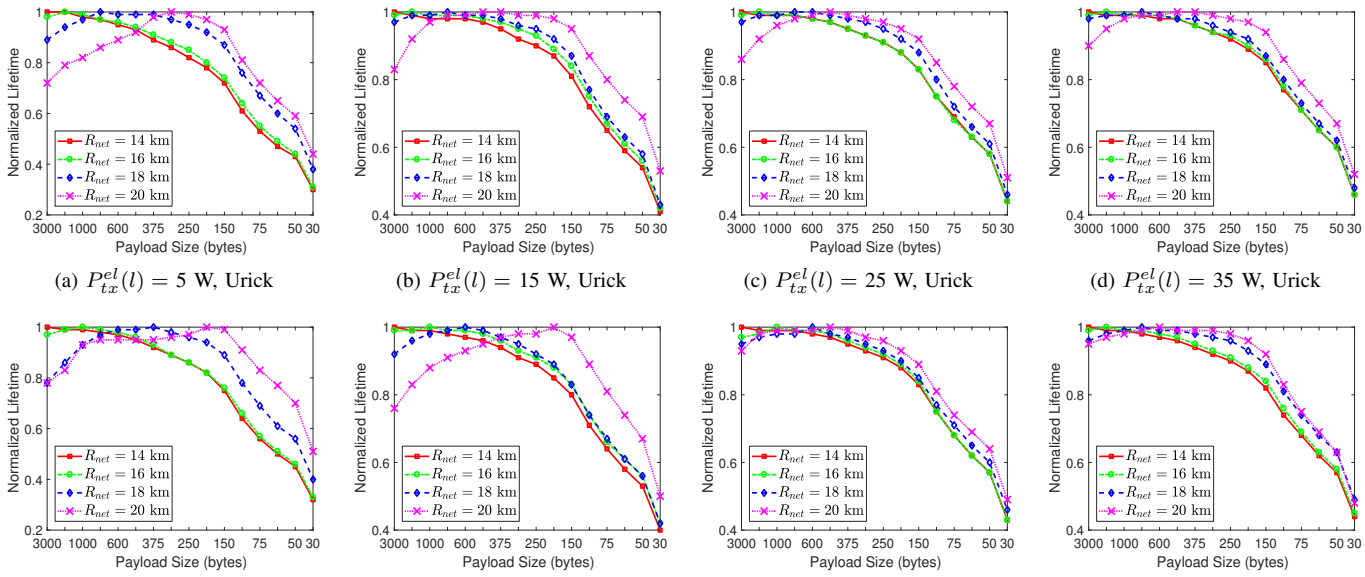

(a) $P_{tx}^{el}(l) = 5$ W, Urick (b) $P_{tx}^{el}(l) = 15$ W, Urick (c) $P_{tx}^{el}(l) = 25$ W, Urick (d) $P_{tx}^{el}(l) = 35$ W, Urick

(e) $P_{tx}^{el}(l) = 5$ W, BELLHOP (f) $P_{tx}^{el}(l) = 15$ W, BELLHOP (g) $P_{tx}^{el}(l) = 25$ W, BELLHOP (h) $P_{tx}^{el}(l) = 35$ W, BELLHOP

Fig. 2: Normalized lifetimes with respect to payload size (in bytes) and network radii (R_{net}) for NL-TPC approach employing Urick and BELLHOP models with global transmission power levels are set to 5, 15, 25, and 35 W throughout the network.

TABLE II: Max. transmit power level-l (max$[P_{tx}^{el}(l)]$ in W), reception power (P_{rx} in W), standby/idle power (P_{std} in mW), central operating frequency (f in kHz), and data rate (R in kbps) of six commercial & research underwater modems [22].

Underwater Modem	max$[P_{tx}^{el}(l)]$ (W)	P_{rx} (W)	P_{std} (mW)	f (kHz)	R (kbps)
EvoLogics S2CR 18/34 WiSE	35	1.3	2.5	26	13.90
WHOI Micromodem	48	3	8	25	5
Teledyne Benthos ATM9XX	20	0.77	16.8	24.50	15.36
LinkQuest UWM4000	7	0.8	8	17	8.50
Aquatech AQUAModem 1000	20	0.6	1	9.75	2
DSPComm AquaComm Marlin	1.8	0.25	1.8	23	0.48

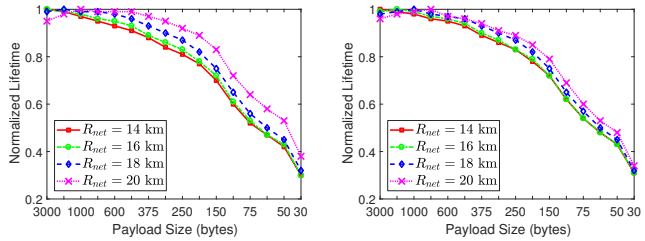

(a) Norm. LT, Urick (b) Norm. LT, BELLHOP

Fig. 3: Normalized lifetimes in terms of seconds with respect to payload size (in bytes) and network radii (R_{net}) for LL-TPC approach employing Urick and BELLHOP models.

18 by $N_R \times R$ and obtain the following inequality

$$\frac{8 \times (L_P + L_A)}{N_R \times R} \times \left(\sum_{j \in V} f_{ij} \lambda_{ij}^{lk} + \sum_{j \in W} \lambda_{ji}^{lk} f_{ji} \right) \leq T_R, \quad \forall i \in V. \tag{22}$$

Note that, right-hand side (RHS) of this modified constraint simply becomes T_R (in seconds) and left-hand side (LHS) of this constraint becomes the amount of time (in seconds) for node-i to transmit and receive data in all directions (including the base station). Our results reveal that the maximum possible network lifetime is around 1 year which is obtained as $N_R = 207360$ rounds when $R_{net} = 14$ km and $L_{PL} = 3000$ bytes for the Urick model. For this configuration, we observe that LHS is 7% of the RHS of the inequality 22. Thus, we can state that the average end-to-end latency is upper bounded by 10.5 seconds.

A. Performance Evaluation of NL-TPC Approach

In this part of the analysis, we present normalized lifetimes for NL-TPC approach as a function payload size and R_{net} values in Figure 2. For each sub-figure of this plot, we fix the global transmission power level on all links to 5, 15, 25, and 35 W, respectively. Upper and lower rows of this figure show results for Urick's and BELLHOP channel models, respectively. In this figure we see that for a dense network (*i.e.*, $R_{net} = 14$ km) regardless of the channel model used, the optimum packet size (OPS) is obtained as 3000 bytes. As we increase R_{net}, the successful handshake probability decreases, thus smaller payload sizes yield maximum lifetime values. When considering a highly sparse network (*i.e.*, high R_{net} values), frames with the maximum payload are quite like

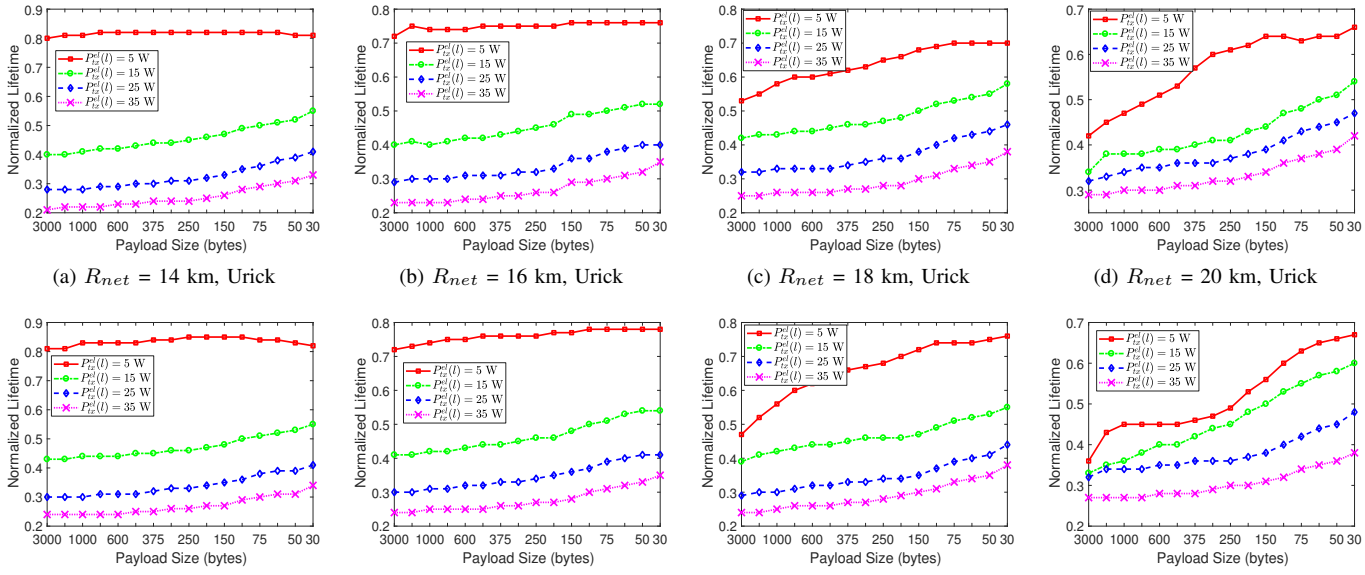

(a) R_{net} = 14 km, Urick (b) R_{net} = 16 km, Urick (c) R_{net} = 18 km, Urick (d) R_{net} = 20 km, Urick

(e) R_{net} = 14 km, BELLHOP (f) R_{net} = 16 km, BELLHOP (g) R_{net} = 18 km, BELLHOP (h) R_{net} = 20 km, BELLHOP

Fig. 4: Normalized network lifetimes for NL-TPC approach with respect to LL-TPC approach as a function of network radii (R_{net} – km), global transmission power levels ($P_{tx}^{el}(l)$ – W) and payload size (bytes) for Urick and BELLHOP models.

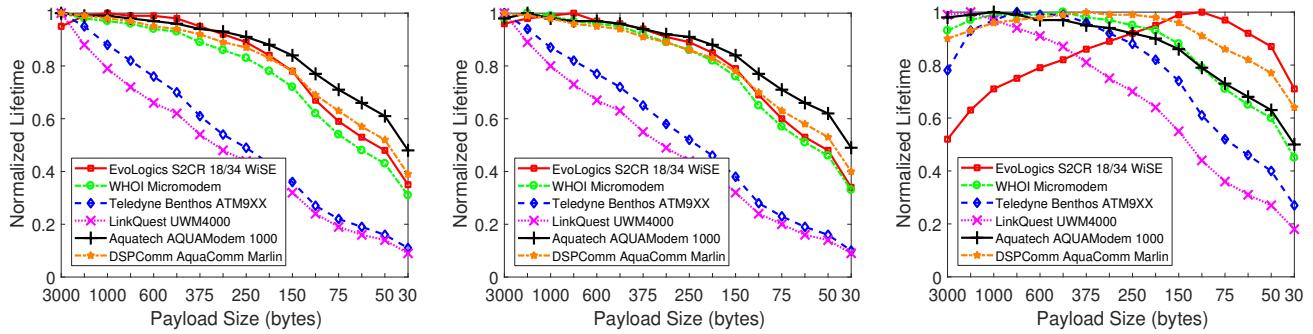

(a) Norm. lifetimes when $h = 500$ m (b) Norm. lifetimes when $h = 1000$ m (c) Norm. lifetimes when $h = 3500$ m

Fig. 5: Normalized network lifetimes for six popular commercial underwater modems and corresponding optimal packet sizes as a function of depth (h) and payload size (bytes) when network radius is set to 20 km ($R_{net} = 20$ km) employing BELLHOP model.

to be dropped. Since a frame drop incurs a retransmission, more energy would be wasted due to the extra transmission which leads lesser lifetime values. That is why lower payloads are preferred to prolong the network lifetime for $R_{net} > 14$ km. Normalized network lifetimes can be reduced to 0.30 (in Figures 2a and 2e) if the smallest payload size (*i.e.*, $L_{PL} = 30$ bytes) and lowest global transmission power level (*i.e.*, $P_{tx}^{el}(l) = 5$ W) is used. For a payload size of 30 bytes, each node would generate 100 packets at each round which results in excessive amount of communication energy dissipation. Hence, the normalized network lifetime rapidly decreases in this case. OPS values obtained for BELLHOP model are smaller than OPS values obtained for Urick's model for sparse networks (*i.e.*, $R_{net} > 18$ km) when we especially consider low global transmission power levels (in Figures 2e and 2f). The reason behind this trend is due to the higher transmission loss values (*i.e.*, A_{ij}) of BELLHOP model. This result becomes visible when the global transmission power levels are low (*i.e.*, $P_{tx}^{el}(l) = 5$ or 15 W). Furthermore, the increment in transmission power positively effects the successful frame reception, hence frames with higher payload sizes yield better normalized lifetimes when compared to the lifetime obtained for the OPS.

B. Performance Evaluation of LL-TPC Approach

In Figures 3a and 3b, we employ LL-TPC approach and aim to determine the OPS values maximizing network lifetimes for each parameter setting. The most striking result emerged from this analysis is that OPS values are different from NL-TPC case which are obtained as 3000, 3000, 1500, and 1000 bytes for Urick's model; 3000, 1500, 1000, and 750 bytes for BELLHOP model considering $R_{net} = 14$, 16, 18, and 20 km, respectively. Since transmission loss

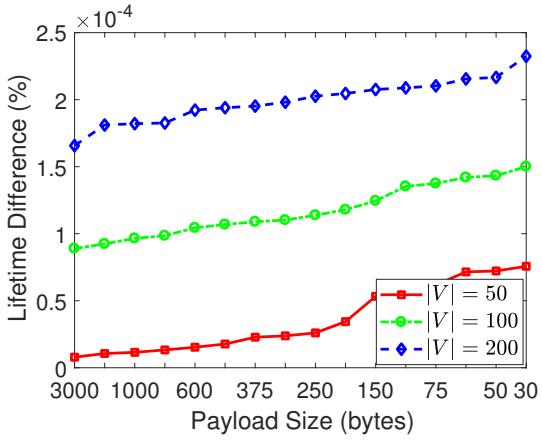

(a) Avg. lifetime differences (%)

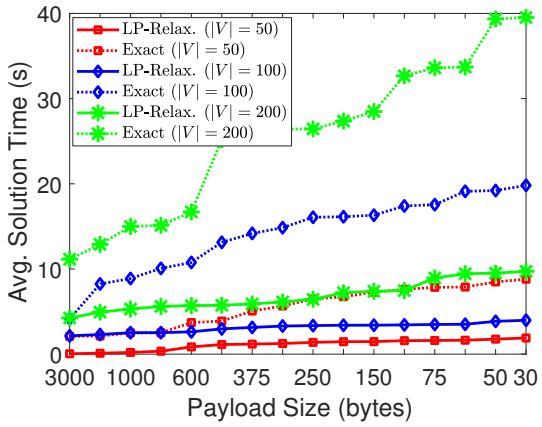

(b) Avg. solution times (s)

Fig. 6: Avg. lifetime differences in percentage between the exact ILP and LP-Relaxation solutions (a) and avg. solution times in seconds (b) as a function of payload size and number of nodes in the network employing BELLHOP model for LL-TPC approach when $R_{net} = 20$ km and and $h = 1000$ m.

values for BELLHOP model are greater than Urick's model, retransmissions occur frequently with the BELLHOP model which forces lower OPS values to be utilized for lifetime maximization. We also observe that payload sizes smaller than 750 bytes are not preferred because LL-TPC approach tries to utilize as minimum as possible transmission power levels on each link individually to guarantee a certain successful handshake probability. Our analysis shows that regardless of the channel model used, average transmission powers (*i.e.*, $[\sum_{(i,j)\in E} l_{ij}^{opt} \times f_{ij}]/\sum_{(i,j)\in E} f_{ij}$) are calculated in the interval 6.00–8.62 W for LL-TPC approach. Similar to the NL-TPC approach, normalized network lifetimes can be reduced to 0.30 if the smallest payload size (*i.e.*, $L_{PL} = 30$ bytes) is used.

C. Comparison of NL-TPC and LL-TPC Approaches

In Figure 4 we present a detailed comparison of normalized network lifetimes for NL-TPC and LL-TPC approaches as a function of R_{net} and payload sizes for both channel models. In this figure, NL-TPC lifetimes are normalized with the LL-TPC lifetimes (LL-TPC lifetimes are taken as 1.00). Regardless of the network size, normalized NL-TPC lifetimes are between 0.42 and 0.82; 0.36 and 0.85 when $P_{tx}^{el}(l) = 5$ W for Urick and BELLHOP models, respectively. As the transmission power increases to 35 W, normalized lifetimes for NL-TPC are in the intervals 0.21–0.42 and 0.23–0.38 for Urick and BELLHOP models, respectively. Utilization of high power levels causes network to dissipate excessive amount of energy hence normalized lifetimes are decreased. As a general trend, normalized lifetimes decrease as the payload size increases due to the wastage of energy for frequent retransmissions when the payload size increases. This result is much visible for highly sparse networks (*e.g.*, $R_{net} > 16$ km).

D. OPS Values of Several Underwater Modems

In this part of the analysis we determine the OPS values for six popular commercial & research underwater modems. Besides the EvoLogics S2CR 18/34 WiSE modem, we choose WHOI Micromodem, Teledyne Benthos ATM9XX, LinkQuest UWM4000, Aquatech AQUAModem 1000, and DSPComm AquaComm Marlin modems which are the most famous underwater modems available in the market and academia. $P_{tx}^{el}(l)$, f, R, P_{rx}, and P_{std} values of these modems are adopted from [22] and reported in Table II. We also quantify the impact of depth on the determination of OPS values for these modems. For this purpose we choose BELLHOP model as the channel model, employ LL-TPC approach (each modem is assumed to have five discrete power levels), fix the network radius to 20 km, and choose depth values as 500, 1000, and 3500 meters. We present the normalized lifetimes with corresponding OPS values in Figure 5 for this parameter configuration. Except for the EvoLogics S2CR 18/34 WiSE modem, OPS values are obtained as 3000 bytes regardless of the modem platform when $h = 500$ m. For this depth, OPS of EvoLogics S2CR 18/34 WiSE modem is observed as 750 bytes. OPS values start to differ as the depth of the network increases. Our results reveal that OPS values can be as high as 1500 bytes (in Figure 5c – LinkQuest UWM4000 modem) and as low as 100 bytes (in Figure 5c – EvoLogics S2CR 18/34 WiSE modem) when $h = 3500$ m.

E. Time Complexity Analysis of the ILP Model

The optimization model that maximizes the network lifetime is an ILP problem which is known to be an NP-complete problem. Since the computation time for NP-complete problems are high, the number of nodes in the network negatively effects the computation time due to the increment of the search space of the f_{ij} integer variable. It is critical to develop some heuristic methods to solve these problems in polynomial time. One of these heuristic methods is known to be Linear Programming (LP) relaxation where the integer variables of the ILP model are taken as continuous variables. LP-relaxation converts the ILP model to LP model and since the LP problems are solved in polynomial time.

We present the lifetime differences (in percentage) and solution times between both with exact integer and LP-relaxation methods in Figure 6a as a function of payload

size and number of EvoLogics S2C 18/34 WiSE nodes in the network (*i.e.*, $|V| = 50$, 100, and 200 nodes) employing BELLHOP model for LL-TPC approach when $R_{net} = 20$ km and $h = 1000$ m. We observe that lifetime difference increases as the payload size decreases however this increment can be neglected since the lifetime difference is in the order of 10^{-5}. Furthermore, as the number of nodes in the network increases, the lifetime difference also increases due to the extra f_{ij} variables included in the ILP model. Nonetheless, we observe that the maximum lifetime difference between the exact and LP-relaxation solution is obtained as 0.00023% (when $|V| = 200$ for $L_{PL} = 30$ bytes). We also observe from Figure 6b that LP-relaxation solutions take significantly lower computation times when compared to exact ILP solutions. Finally, as the number of nodes in the network increases the solution times for both exact ILP and LP-relaxation increases but we can say that the maximum solution time for the LP-relaxation approach does not exceed 10 seconds. Finally, our analysis reveals that choice of different modem platforms has insignificant effects on the results.

V. Conclusion

In this work, a realistic link-layer energy consumption abstraction for UASNs is proposed by using the power consumption characteristics of the EvoLogics S2C 18/34 WiSE underwater acoustic node platform which sits on top of two different acoustic propagation models (*i.e.*, an empirical approximate model and accurate underwater propagation tool which can perform ray tracing). We also propose an optimization framework via ILP to jointly optimizes transmission power and frame size to maximize the network lifetime. We construct two TPC approaches by using the proposed optimization model. We perform our analysis in a wide range of parameter space (*e.g.*, node density, transmission power, *etc.*). We further determine optimal frame sizes for several underwater modems and provide a time complexity analysis of the optimization framework. Our main conclusions are itemized as follows:

1) There exists an optimal frame size where the network lifetime can be maximized which depends on the channel conditions, network density, underwater modem platform, and TPC approach that is employed.
2) For successful handshake probabilities greater than 0.23, the optimum frame size would be as highest as possible to reduce the extra transmission energy costs due to the retransmissions and fragmentation. As the underwater channel conditions become much worse smaller frames which are prone to frame drops yield a maximized network lifetime.
3) Although NL-TPC scheme is easy to be implemented in UASNs, such an approach may underestimate the network lifetime at least 18% when compared to LL-TPC approach due to the wastage of energy dissipation.
4) Determination of optimal packet sizes should be decided jointly with the transmission power control approaches in order to maximize the network. The optimum frame size that yields a maximized lifetime for NL-TPC approach may not be suitable for LL-TPC approach.
5) Joint optimization of packet size and transmission power has never been incorporated into any practical underwater acoustic communication applications, possibly, due to the lack of the analysis to determine the effects of such optimization on system performance. However, our results which address the gap in the literature, clearly, reveal that joint optimization of packet size and transmission power has a significant impact on network lifetime optimization in UASNs. Therefore, future practical UASN architects must incorporate joint optimization of packet size and transmission power in their designs.

Future work includes extending the proposed optimization framework by jointly optimizing the operating frequency, TPC approach, and packet size for various UASN applications.

Acknowledgement

The work of V. C. Gungor is supported by TUBITAK 1001 Project (project no. 114E248).

References

[1] I. F. Akyildiz, D. Pompili, and T. Melodia, "Underwater acoustic sensor networks: research challenges," *Ad Hoc Networks*, vol. 3, no. 3, pp. 257–279, 2005.
[2] J. Jiang, G. Han, L. Shu, S. Chan, and K. Wang, "A trust model based on cloud theory in underwater acoustic sensor networks," *IEEE Trans. Industrial Informatics*, vol. 13, no. 1, pp. 342–350, 2017.
[3] S. Basagni, C. Petrioli, R. Petroccia, and M. Stojanovic, "Optimized packet size selection in underwater wireless sensor network communications," *IEEE Journal of Oceanic Engineering*, vol. 37, no. 3, pp. 321–337, 2012.
[4] T. M. Chiwewe and G. P. Hancke, "A distributed topology control technique for low interference and energy efficiency in wireless sensor networks," *IEEE Trans. Industrial Informatics*, vol. 8, no. 1, pp. 11–19, 2012.
[5] X. Jin, Y. Chen, and X. Xu, "The analysis of hops for multi-hop cooperation in underwater acoustic sensor networks," in *Proc. IEEE/OES China Ocean Acoustics (COA)*, 2016, pp. 1–5.
[6] Z. Zhou, W. Fang, J. Niu, L. Shu, and M. Mukherjee, "Energy-efficient event determination in underwater WSNs leveraging practical data prediction," *IEEE Trans. Industrial Informatics*, vol. 13, no. 3, pp. 1238–1248, 2017.
[7] G. Tuna and V. C. Gungor, "A survey on deployment techniques, localization algorithms, and research challenges for underwater acoustic sensor networks," *International Journal of Communication Systems*, pp. e3350–n/a, 2017.
[8] M. Stojanovic, "Optimization of a data link protocol for an underwater acoustic channel," in *Proc. Europe Oceans*, vol. 1, 2005, pp. 68–73.
[9] M. Ayaz, L. T. Jung, A. Abdullah, and I. Ahmad, "Reliable data deliveries using packet optimization in multi-hop underwater sensor networks," *Journal of King Saud University - Computer and Information Sciences*, vol. 24, no. 1, pp. 41–48, 2012.
[10] M. C. Vuran and I. F. Akyildiz, "Cross-layer packet size optimization for wireless terrestrial, underwater, and underground sensor networks," in *Proc. IEEE Conf. Computer Communications (INFOCOM)*, 2008.
[11] W. Ahmad, K. M. Awan, and K. Iqbal, "Dynamic length packet size communication technique for underwater sensor networks," in *Proc. Int. Conf. Intelligent Systems Engineering (ICISE)*, 2016, pp. 242–249.
[12] M. Molins and M. Stojanovic, "Slotted FAMA: a MAC protocol for underwater acoustic networks," in *Proc. OCEANS - Asia Pacific*, 2006, pp. 1–7.
[13] X. Guo, M. R. Frater, and M. J. Ryan, "A propagation-delay-tolerant collision avoidance protocol for underwater acoustic sensor networks," in *Proc. OCEANS - Asia Pacific*, 2006, pp. 1–6.
[14] H. U. Yildiz, B. Tavli, and H. Yanikomeroglu, "Transmission power control for link-level handshaking in wireless sensor networks," *IEEE Sensors Journal*, vol. 16, no. 2, pp. 561–576, 2016.
[15] D. Pompili, T. Melodia, and I. F. Akyildiz, "A CDMA-based medium access control for underwater acoustic sensor networks," *IEEE Trans. Wireless Communications*, vol. 8, no. 4, pp. 1899–1909, 2009.

[16] A. Castagnetti, A. Pegatoquet, T. N. Le, and M. Auguin, "A joint duty-cycle and transmission power management for energy harvesting WSN," *IEEE Trans. Industrial Informatics*, vol. 10, no. 2, pp. 928–936, 2014.
[17] E. M. Sozer, M. Stojanovic, and J. G. Proakis, "Underwater acoustic networks," *IEEE Journal of Oceanic Engineering*, vol. 25, no. 1, pp. 72–83, 2000.
[18] P. Xie and J. H. Cui, "Exploring random access and handshaking techniques in large-scale underwater wireless acoustic sensor networks," in *Proc. OCEANS*, 2006, pp. 1–6.
[19] H. H. Ng, W. S. Soh, and M. Motani, "MACA-U: A media access protocol for underwater acoustic networks," in *Proc. IEEE Global Telecommunications Conference (GLOBECOM)*, 2008, pp. 1–5.
[20] M. B. Porter and H. P. Bucker, "Gaussian beam tracing for computing ocean acoustic fields," *The Journal of the Acoustical Society of America*, vol. 82, no. 4, pp. 1349–1359, 1987.
[21] M. Stojanovic, "On the relationship between capacity and distance in an underwater acoustic communication channel," in *Proc. ACM Int. Workshop on Underwater Networks (WUWNet)*, 2006, pp. 41–47.
[22] S. Sendra, J. Lloret, J. M. Jimenez, and L. Parra, "Underwater acoustic modems," *IEEE Sensors Journal*, vol. 16, no. 11, pp. 4063–4071, 2016.
[23] A. Akbas, H. U. Yildiz, and B. Tavli, "Data packet length optimization for wireless sensor network lifetime maximization," in *Proc. Int. Conf. Communications (COMM)*, 2014, pp. 1–6.
[24] A. Akbas, H. U. Yildiz, B. Tavli, and S. Uludag, "Joint optimization of transmission power level and packet size for wsn lifetime maximization," *IEEE Sensors Journal*, vol. 16, no. 12, pp. 5084–5094, 2016.
[25] M. C. Oto and O. B. Akan, "Energy-efficient packet size optimization for cognitive radio sensor networks," *IEEE Trans. Wireless Communications*, vol. 11, no. 4, pp. 1544–1553, 2012.
[26] K. S. Deepak and A. V. Babu, "Packet size optimization for energy efficient cooperative wireless body area networks," in *Proc. IEEE India Conference (INDICON)*, 2012, pp. 736–741.
[27] S. Kurt, H. U. Yildiz, M. Yigit, B. Tavli, and V. C. Gungor, "Packet size optimization in wireless sensor networks for smart grid applications," *IEEE Trans. Industrial Electronics*, vol. 64, no. 3, pp. 2392–2401, 2017.
[28] D. Pompili, T. Melodia, and I. F. Akyildiz, "Routing algorithms for delay-insensitive and delay-sensitive applications in underwater sensor networks," in *Proc. Int. Conf. Mobile Computing and Networking (MobiCom)*, 2006, pp. 298–309.
[29] S. Basagni, C. Petrioli, R. Petroccia, and M. Stojanovic, "Choosing the packet size in multi-hop underwater networks," in *Proc. IEEE OCEANS - Sydney*, 2010, pp. 1–9.
[30] ——, "Optimizing network performance through packet fragmentation in multi-hop underwater communications," in *Proc. IEEE OCEANS - Sydney*, 2010, pp. 1–7.
[31] L. T. Jung and A. B. Abdullah, "Underwater wireless network energy efficiency and optimal data packet size," in *Proc. Int. Conf. Electrical, Control and Computer Engineering (InECCE)*, 2011, pp. 178–182.
[32] T. Nguyen, T. M. Hoang, and T. N. Lang, "A study on link quality in single hop sensor networks with brownian motion," in *Proc. Int. Conf. Recent Advances in Signal Processing, Telecommunications Computing (SigTelCom)*, 2017, pp. 235–239.
[33] K. S. Geethu and A. V. Babu, "Energy optimal channel attempt rate and packet size for ALOHA based underwater acoustic sensor networks," *Telecommunication Systems*, vol. 65, no. 3, pp. 429–442, 2017.
[34] V. Rodoplu and M. K. Park, "An energy-efficient MAC protocol for underwater wireless acoustic networks," in *Proc. MTS/IEEE OCEANS*, vol. 2, 2005, pp. 1198–1203.
[35] EvoLogics. Underwater acoustic modem S2CR 18/34 white line science edition (WiSE) product information. [Online]. Available: https://www.evologics.de/files/DataSheets/EvoLogics_S2CR_1834_WiSE_Product_Information.pdf
[36] R. Su, R. Venkatesan, and C. Li, "Balancing between robustness and energy consumption in underwater acoustic sensor networks," in *Proc. IEEE Wireless Communications and Networking Conference (WCNC)*, 2015, pp. 1048–1053.
[37] M. Zorzi, P. Casari, N. Baldo, and A. F. Harris, "Energy-efficient routing schemes for underwater acoustic networks," *IEEE Journal on Selected Areas in Communications*, vol. 26, no. 9, pp. 1754–1766, 2008.
[38] S. Gul, S. S. H. Zaidi, R. Khan, and A. B. Wala, "Underwater acoustic channel modeling using BELLHOP ray tracing method," in *Proc. International Bhurban Conf. Applied Sciences and Technology (IBCAST)*, 2017, pp. 665–670.
[39] C. Petrioli, R. Petroccia, J. R. Potter, and D. Spaccini, "The SUNSET framework for simulation, emulation and at-sea testing of underwater wireless sensor networks," *Ad Hoc Networks*, vol. 34, pp. 224–238, 2015.
[40] R. Masiero, S. Azad, F. Favaro, M. Petrani, G. Toso, F. Guerra, P. Casari, and M. Zorzi, "DESERT underwater: An NS-Miracle-based framework to design, simulate, emulate and realize test-beds for underwater network protocols," in *Proc. IEEE Oceans - Yeosu*, 2012, pp. 1–10.
[41] S. R. Thompson, "Sound propagation considerations for a deep-ocean acoustic network," Ph.D. dissertation, Naval Postgraduate School, Monterey, California, 2009.
[42] J. Llor and M. P. Malumbres, "Statistical modeling of large-scale signal path loss in underwater acoustic networks," *Sensors*, vol. 13, no. 2, pp. 2279–2294, 2013.
[43] E. M. Rubino, D. Centelles, J. Sales, J. V. Marti, R. Marin, P. J. Sanz, and A. J. Alvares, "Progressive image compression and transmission with region of interest in underwater robotics," in *Proc. OCEANS 2017 - Aberdeen*, 2017, pp. 1–9.
[44] L. Hong, F. Hong, Z. W. Guo, and X. Yang, "A TDMA-based MAC protocol in underwater sensor networks," in *Proc. Int. Conf. Wireless Communications, Networking and Mobile Computing*, 2008, pp. 1–4.
[45] EvoLogics. S2C battery packs. [Online]. Available: https://www.evologics.de/en/products/Accessories/s2cr_battery_packs.html
[46] A. Stefanov and M. Stojanovic, "Design and performance analysis of underwater acoustic networks," *IEEE Journal on Selected Areas in Communications*, vol. 29, no. 10, pp. 2012–2021, 2011.

Huseyin Ugur Yildiz (S'13—M'16) received the B.S. degree from Bilkent University, Ankara, Turkey, in 2009, and the M.S. and Ph.D. degrees from TOBB University of Economics and Technology, Ankara, Turkey, in 2013 and 2016, respectively, all in electrical and electronics engineering. He is an Assistant Professor in the Department of Electrical and Electronics Engineering at TED University, Ankara, Turkey. His research focuses on the applications of optimization techniques for modeling and analyzing research problems on wireless communications, wireless networks, underwater acoustic networks, and smart grids.

Vehbi Cagri Gungor received his B.S. and M.S. degrees in Electrical and Electronics Engineering from Middle East Technical University, Ankara, Turkey, in 2001 and 2003, respectively. He received his Ph.D. degree in electrical and computer engineering from the Broadband and Wireless Networking Laboratory, Georgia Institute of Technology, Atlanta, GA, USA, in 2007. Currently, he is an Associate Professor and Chair of Computer Engineering Department, Abdullah Gul University (AGU), Kayseri, Turkey. His current research interests are in next-generation wireless networks, wireless ad hoc and sensor networks, smart grid communications, and underwater networks.

Bulent Tavli (S'97—M'05–SM'17) received the B.S. degree in electrical and electronics engineering from Middle East Technical University, Ankara, Turkey, in 1996, and the M.S. and Ph.D. degrees in electrical and computer engineering from the University of Rochester, Rochester, NY, USA, in 2002 and 2005, respectively. He is a Professor with the Department of Electrical and Electronics Engineering, TOBB University of Economics and Technology, Ankara. His current research interests include wireless communications, networking, optimization, embedded systems, information security, and smart grids.